Finite difference elastic modeling of the topography and the weathering layer

Saul E. Guevara and Gary F. Margrave

ABSTRACT

Finite difference 2D elastic modeling is used to study characteristics of the wave field originated by the near surface and the topography. A number of geological models, from flat horizontal to a real topography from a rough setting are presented and results of variation in velocities and waveforms are compared for a number of cases with and without a near surface low velocity layer. It can b noticed that many coherent noise events are generated in the low velocity near surface layer. Many of them resemble real data seismograms. Some of them are rarely observed in real data and could be related to the characteristics of the algorithm or perhaps to unrealistic velocity models. The surface waves appear dispersive and/or weaker in the presence of topography. Converted waves appear distorted and difficult to identify on some seismograms, mostly due to this coherent noise. The real topography model shows noisy events not clearly defined, which can be related to the dispersion caused by the topography.

INTRODUCTION

The near surface, also known as NSL (for Near Surface Layer) has different characteristics compared with deeper rocks, which affects wave propagation. Land seismic data, recorded at the earth surface, results from waves that travel through the weathering layer, and is sometimes recorded on rough terrain; consequently the image of deeper layers suffers distortion. Many authors have pointed out the near surface as a main shortcoming for seismic methods, especially at some locations on land, such as rough terrain (e. g. Cox, 1999). This drawback is even more critical for shear waves, as has been noticed by some authors (e. g. Anno, 1987; Garotta, 2000).

Seismic modeling is a technique that allows studying the response of the wave propagation to the medium properties. In this way it is possible to understand the characteristics of real seismograms, to develop hypotheses about the media properties and to try methods to improve the image of geological formations. Among the wave modeling methods, finite-difference is favored for some research applications because of its accuracy and its simplicity of computer implementation.

A finite-difference elastic 2-D program is used in this work. It is based on the Levander, (1988) staggered grid 4th order in space 2nd order in time algorithms, which have been enhanced to include the topography characteristics and variable grid (for computer efficiency) according to Hayashi et al, (2000). It allows simulation of many properties of the near surface, such as velocity variation and topography. Properties of rocks such as inelastic and anisotropic behavior are not considered in this algorithm.

The near surface layer is affected by weathering, and the velocity of P and S-waves is in general much lower compared to the intact rock, can change in a short lateral distance, and its thickness can also vary. Molotova and Vassiliev (1960) presented a model of this layer for P and S-wave velocities, where the V_p/V_s is high (>3) in the near surface, and much lower at the parental rock, with some increase related to the water table. The NSL variations generally depend on the parental rock, the latitude and weather, and some other environmental variables. In order to understand the characteristics of real seismograms, topography should also be considered.

Examples of these characteristics are presented and analyzed in this work. In this way it is possible to obtain information about effects such as the change of direction of the particle displacement in the near surface, the relation between the wavelength and the layer thickness, and between coherent noise and signal obtained. Real cases would include all the factors mentioned simultaneously, but for research purposes it is required to try to separate each of them. Cases are presented in a sequence from the simpler to a real digitized topography.

METHODOLOGY

The goals of this work include investigation of a number of issues such as:

- Effect of the slope
- Effect of the thickness of the NSL
- Variations in the velocity properties of the NSL.
- Characteristics of the reflected P-wave and S-wave

The most important finite-difference limitation is related to the computer resources required, which depend on the grid size. The grid size and time step depend on the velocity field of the model, and on the frequency content of the wavelet selected (Levander, 1988). Figure 1 illustrates the wavelet used for most of the examples presented here, a symmetrical Ricker wavelet whose dominant frequency is about 50 Hz.. Figure 1a is the wavelet in the time domain, and Figure 1b is the corresponding amplitude spectrum.

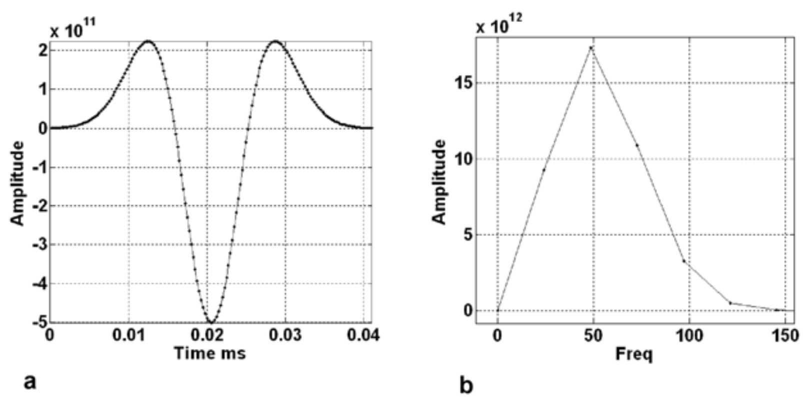

FIG. 1. (a) Ricker wavelet used for the FD modeling and (b) its amplitude spectrum.

Models of increasing complexity are presented. A model without a NSL is included for all the cases, to study how the reflected waves can be affected by the overburden complexity. The topography is assumed flat for the initial models, and its roughness increases in four examples until a last case with real topography. The four models presented are:

1. Horizontal surface.
2. Flat surface with slope.
3. A simple topography
4. Real topography.

The parameters selected are a trade-off between the real properties observed in rocks and reasonable computer requirements for calculation. The near surface layer velocity: is about 1000 m/s for P-wave and about 500 m/s for S-wave. The second layer velocity is about 2000 m/s. The thickness of the near surface was usually around 40 m. For a 50 Hz frequency and a near surface velocity of 1000 m/s the wavelength will be 20 m, and for a 50 Hz frequency and a near surface velocity of 500 m/s the wavelength will be 10 m. So the thickness of the near surface layer is only a few wavelengths at the dominant frequency.

The source of energy is located at about 20 m below the surface. It is a dilatational source, which is generated by normal stresses at the source location. Consequently it is a P-wave source in principle.

RESULTS

Model 1: Horizontal surface

The horizontal surface allows identification of some features related to the presence of a low velocity layer without any topography. Two model variations were used: one without a low velocity near surface, and the other with it. A sketch of the model characteristics and dimensions for the second case is illustrated in Figure 2. The width is 2000 m and the height is 500 m, with a thickness of 40 m for the NSL and a reflector at 250. The velocities used are in Table 1.

Table 1. Velocities and densities of the model 1.

Layer	**Thickness at the SP**	**Vp (m/s)**	**Vs (m/s)**	**Density (Kg/m^3)**
1	5	0	0	0
2: NSL	40	800	400	2000
3	210	2000	1000	2400
4	250	2800	1400	2400

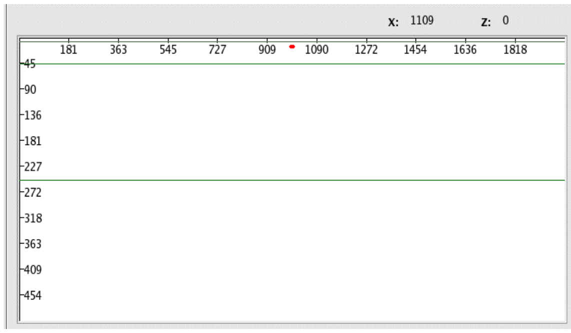

FIG. 2. Model 1: A flat horizontal surface. The P-wave velocities for the layers are in Table 1. The thicknesses are 40 for the NSL and 260 for the second layer. The shot location is marked by a red dot in the middle, close to the surface. A similar model without a NSL was used for comparison.

Figure 3 show the resulting seismograms (vertical component to the left and horizontal component to the right) without a NSL and Figure 4 the corresponding seismograms with NSL. Linear events can be observed in Figure 3, the first one corresponding to refractions and the second one to surface waves; and hyperbola-shape events corresponding to the P-wave, the PS (Converted) wave and the S-wave reflections. Figure 4 events are much more difficult to identify possibly because the surface waves are complex and dispersive. Multiple reflections probably related to the near surface are also present. The high impedance for the base of the weathering layer assumed in the model (about 0.4) is the main reason for the high energy of these events.

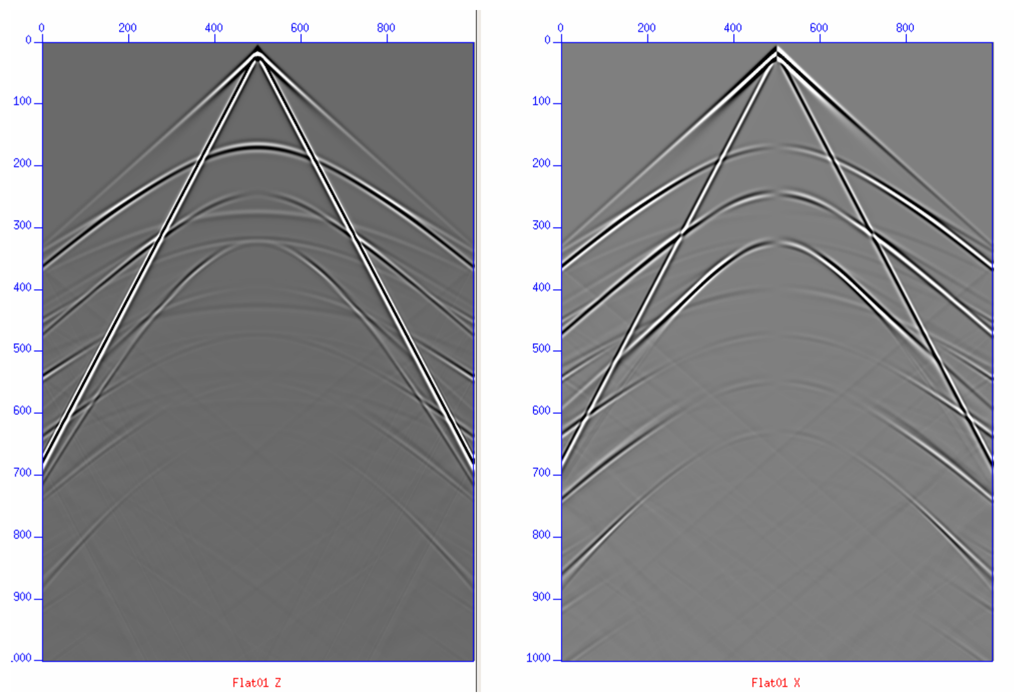

FIG. 3. Model 1 without a LVL.

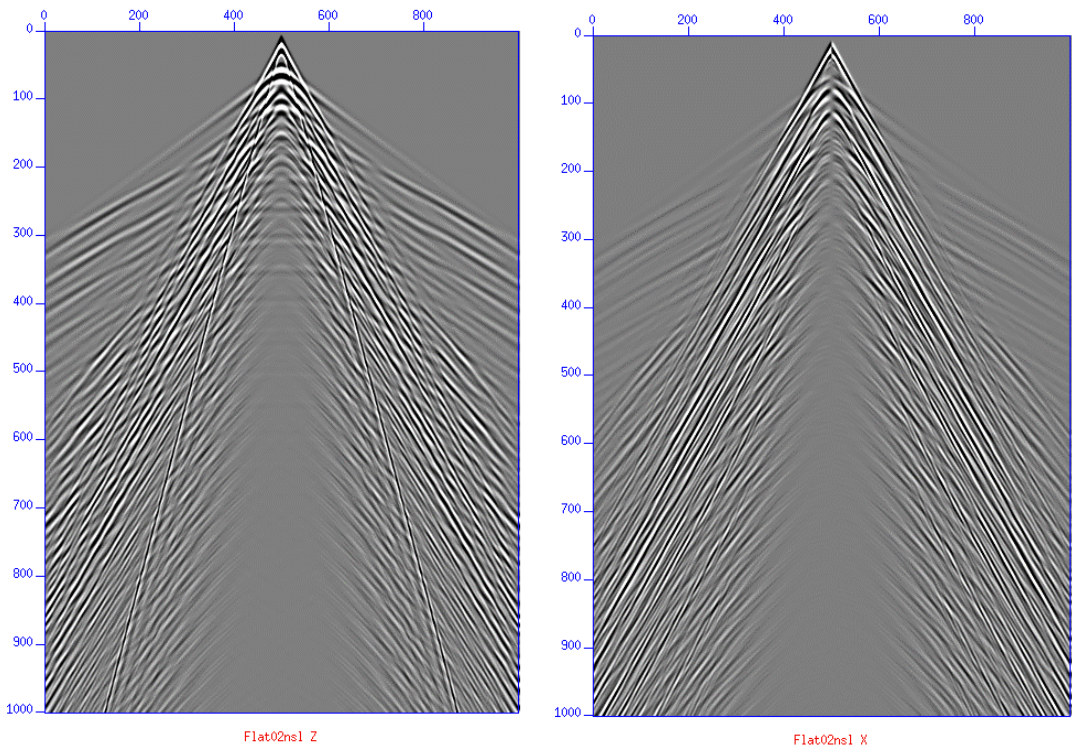

FIG. 4. Model 1 the Vertical component (left) and the horizontal component (right) seismograms. Compare the noisy events here with Figure 6.

Model 2: A flat sloping topography.

Figure 5 illustrates the flat sloping topography including a NSL of low velocity. As before, a similar model without a NSL is also presented. The velocities in Figure 5 are 1000, 1800 and 2400 m/s and the Vp/Vs ratio is 2. The surface slope is 14°. The impedance of the NSL-rock is about 0.3, lower than in model 1. The source of energy is located in the middle of the model, close to the surface.

Figure 6 illustrates the seismograms for the flat slope without NSL and Figure 7 the seismograms with NSL. Asymmetry in the reflections s observed in Figures 6 and 7. Also asymmetry in the surface waves can be observed in Figure 6, which could be related to the features of the algorithm. Dispersive noise can be noticed in Figure 7. The main reflection events are closely corresponding in Figures 6 and 7; however, differences in their amplitudes and in their amplitude variation with offset can be seen.

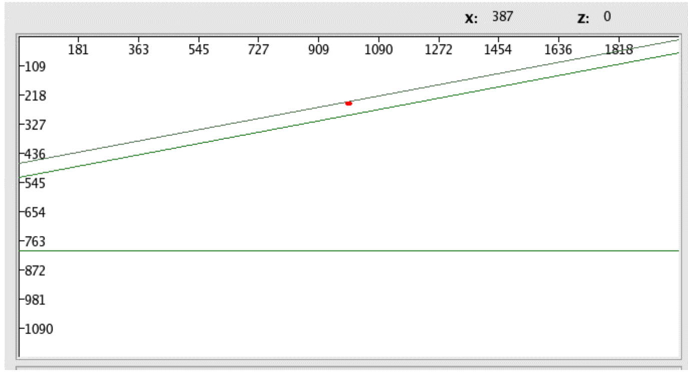

FIG. 5. Model 2: A flat slope of 14° over a horizontal reflector.

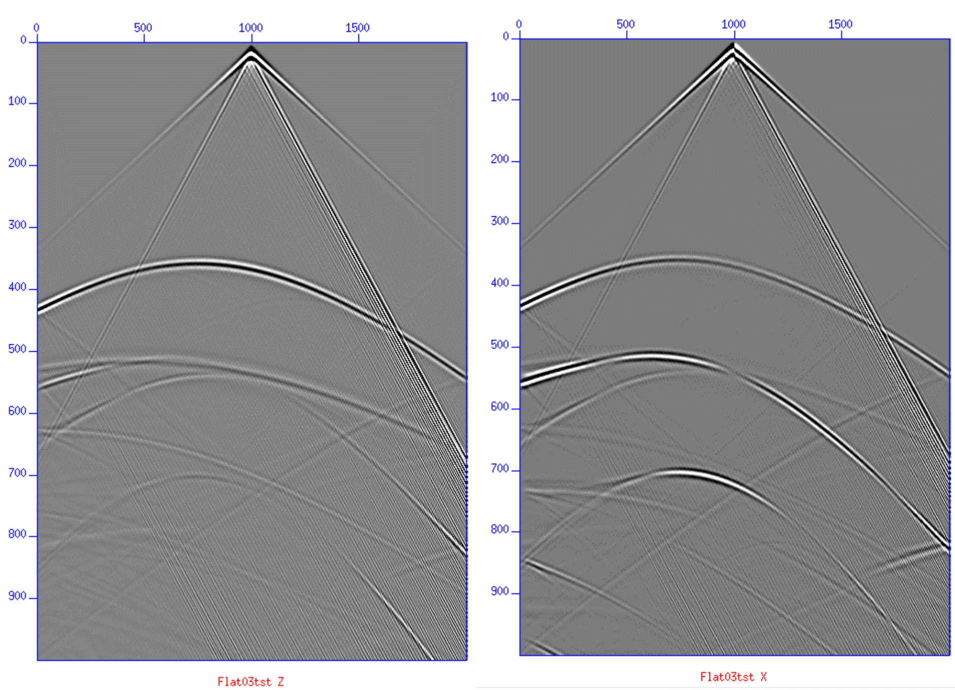

FIG. 6. Dipping layer without a low velocity NSL.

Model 3: Simple topography

Figure 8 illustrates a model with topography variations. From left to right there are two gentle slopes (about 15 °) after the flat and a steep slope of about 45° before the last flat. The NSL is divided into three smaller layers, each one with about 15 m thickness, to mimic a slowly varying NSL: The properties of the layers, including the Free Air, are illustrated in Table 2. Layers 2, 3 and 4 correspond to the NSL.

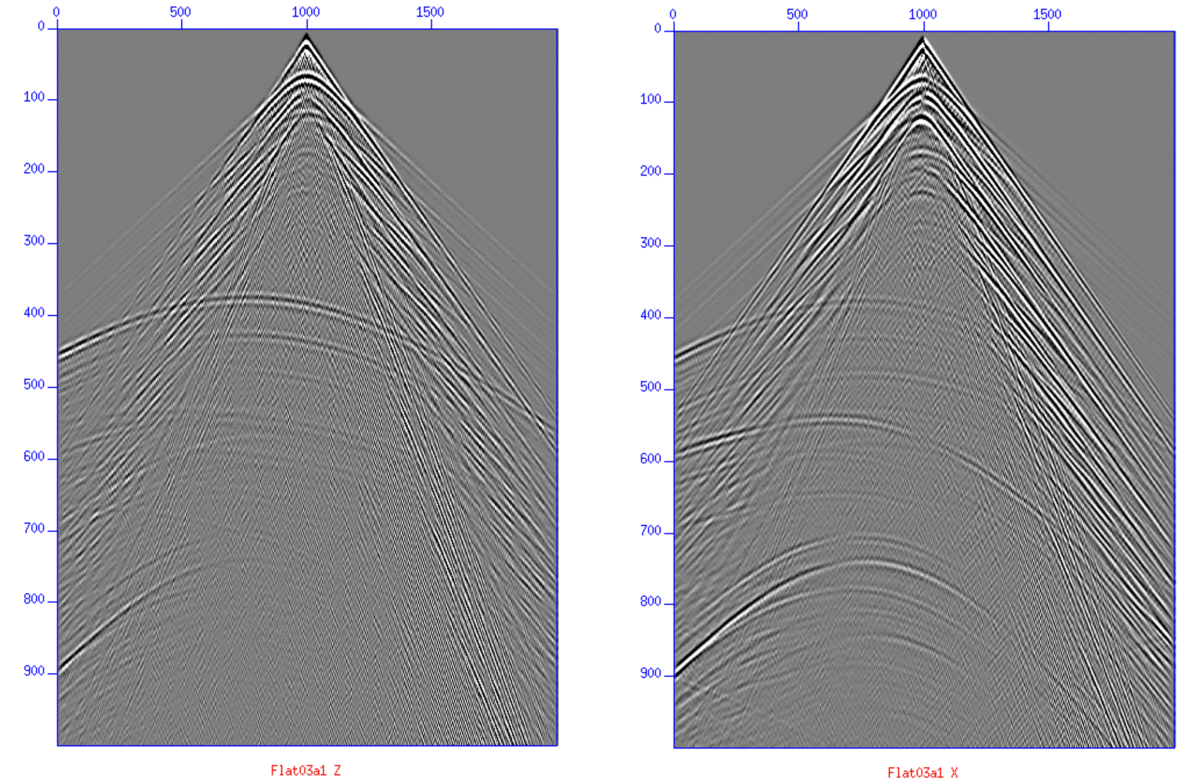

FIG. 7. Model with low velocity near surface layer and with slope in the surface. Vertical and horizontal components. Compare with Figure 6.

Table 2. Velocities and densities of the model 3.

Layer	**Thickness at the SP(m)**	**Vp (m/s)**	**Vs (m/s)**	**Density (Kg/m^3)**
1	10	0	0	0
2:	15	1000	250	2100
3:	15	1250	300	2200
4:	15	1500	500	2300
5	440	1750	1000	2400
6	500	2500	1250	2500

Figures 9 and 10 show the seismograms without and with the NSL. Similar reflection events can be seen in both cases. However more multiples and surface generated noise are observed in the NSL case. This noise appears relatively stronger in the horizontal component. Figure 11 is a snapshot of the vertical component of Fig. 10 at 450 ms, which corresponds to the time sample 225. Noisy events at the x-coordinate 400 can be identified on both. It can be seen that this event is related to near surface guided waves originating near a slope change. This type of event becomes stronger at later time, and eventually makes it quite difficult to identify converted wave events in the horizontal component (Figure 10, right).

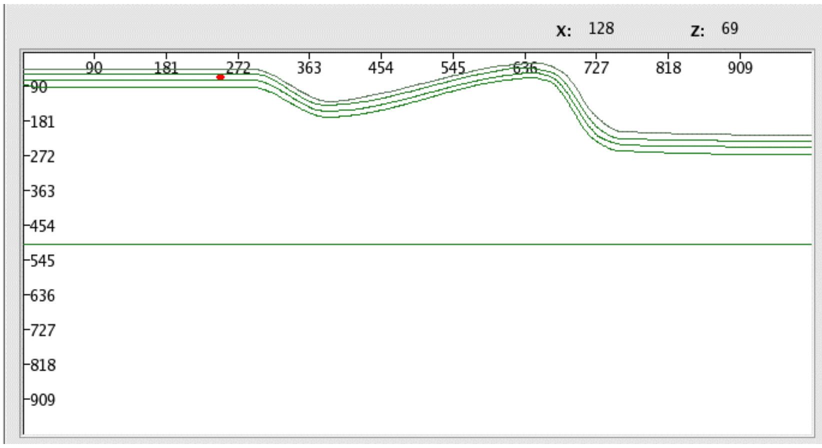

FIG. 8. Model 3: A topography model. This is the model with a NSL. This NSL is divided into three sub-layers, in order to simulate a slowly varying NSL:

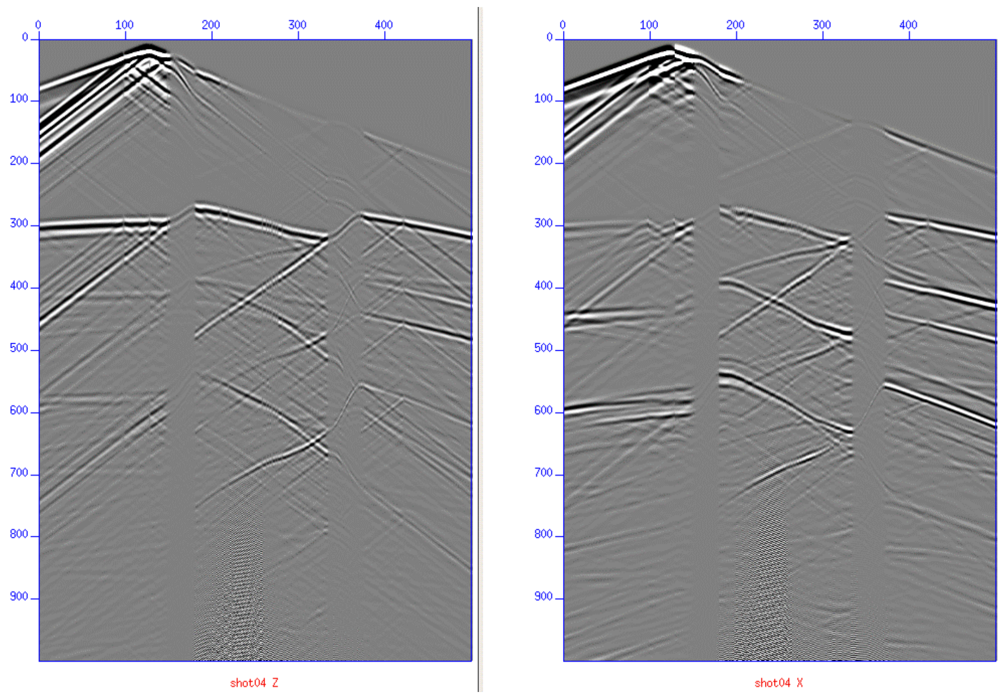

FIG. 9. Model of a variable topography without a near-surface low velocity layer.

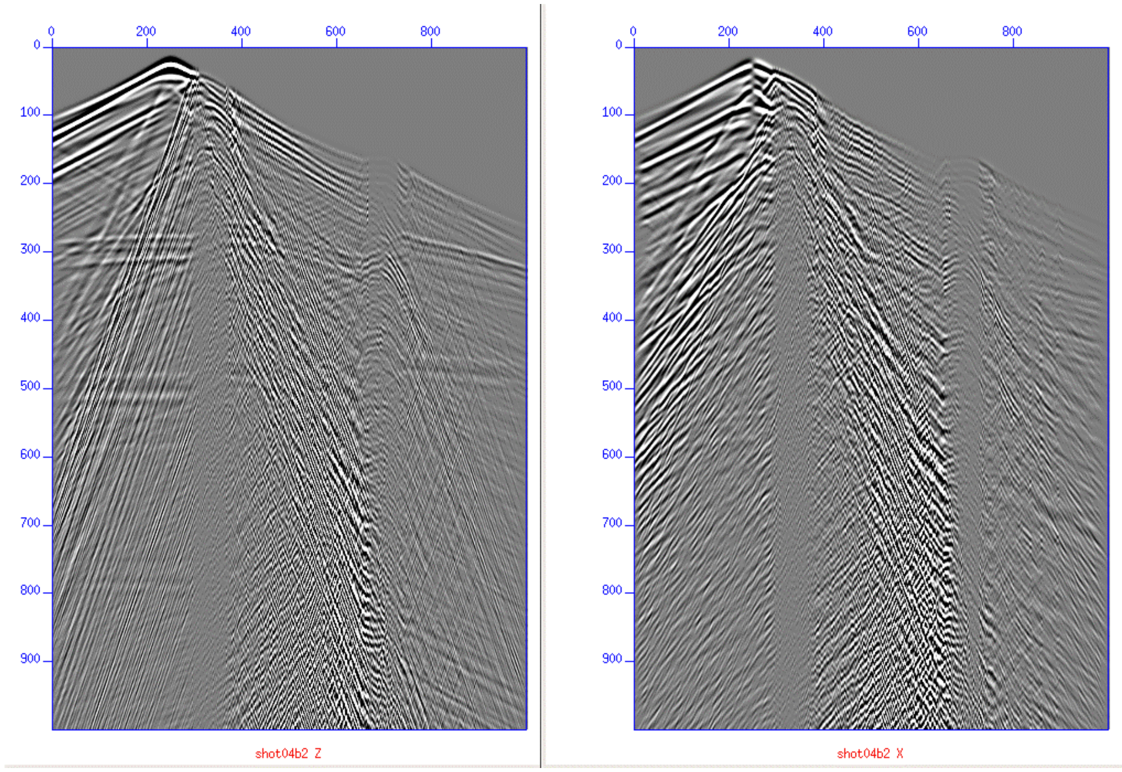

FIG. 10. Seismogram with topography.and a NSL variable in the Z-direction (vertical).

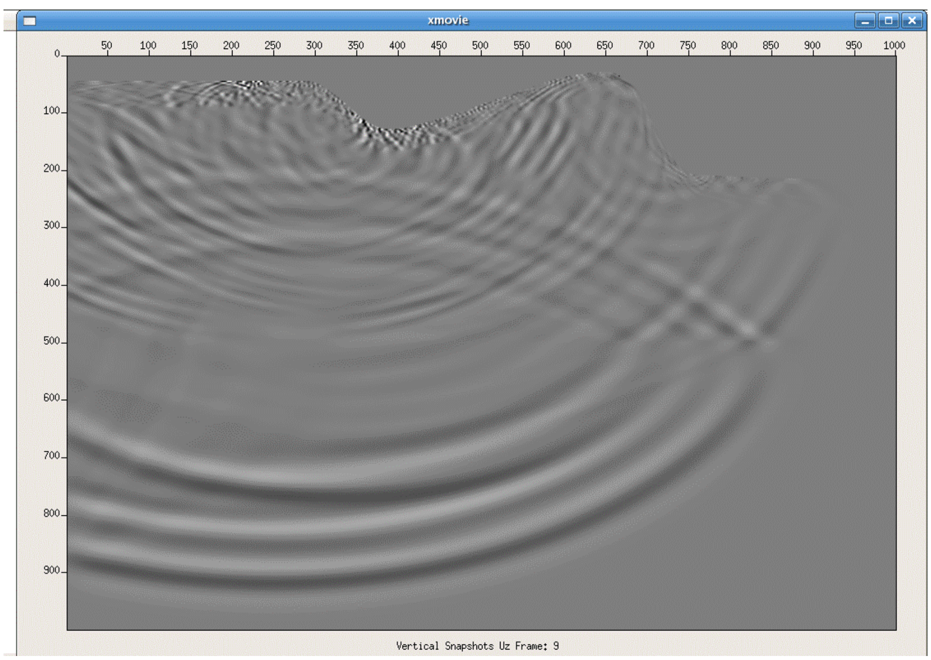

FIG. 11. Snapshot of Model 3, vertical component, corresponding to 450 ms. Notice the near surface events, which include guided waves and perhaps artifacts related to discretization and change of slope (in the middle section, x-location 400).

Case 4: Real topography

This example corresponds to real topography from a seismic multicomponent survey acquired in Colombia in a mountainous setting. This is a place of complex geology with outcrops from different formations, and intermittent rough topography. Figure 12 illustrates the model used here. The horizontal size of the model is 5000 m and its depth 1000 m. The velocities selected are in Table 3. As in the other models, a model without a NSL was also tested. The results of this model without a NSL are in Figure 13 and the results of the model with a NSL are in Figure 14. The record time is 2 seconds, and the time numbering corresponds to samples (2 ms sampling time).

As shown by Figure 13, topography affects the reflection arrivals, and some events are generated by its roughness. Both P-waves and S-waves appear in both components; however their shape and amplitude show complex variations. On the other hand, as shown by Fig. 14, amplitudes are also affected by the near surface layer and the reflection has a different character compared with Fig. 13. However, it is possible to identify P-waves and S-waves in both components. Horizontal variation in amplitudes for the same event in Fig. 14 compared to Fig. 13 can be related to near surface direction variation, that is to say, polarization direction change caused by the near surface layer. It appears that the rough topography does not support the establishment of a strong surface wave.

Table 3. Velocities and densities of Model 4.

Layer	Thickness at theSP (m)	Vp (m/s)	Vs (m/s)	Density (Kg/m^3)
1	110	0	0	0
2: NSL	40	1000	500	2000
3	600	1500	750	2400
4	150	2000	1000	2400

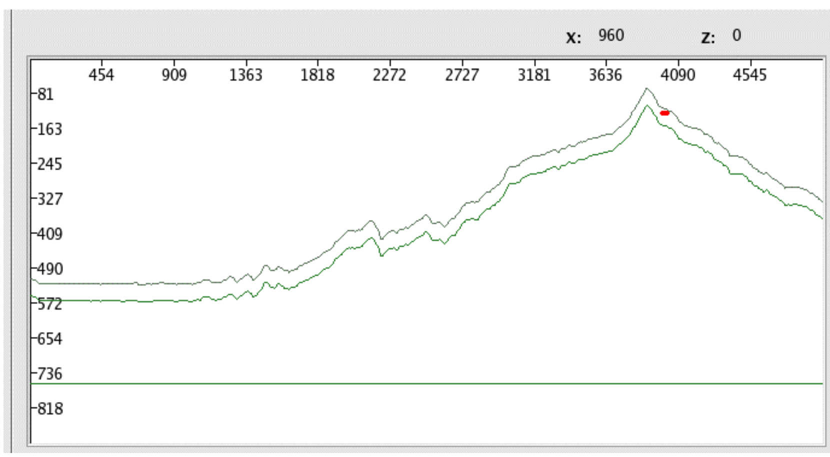

FIG. 12. Model 4: the real topography with a low velocity NSL. The source is located about the distance x=4000 m.

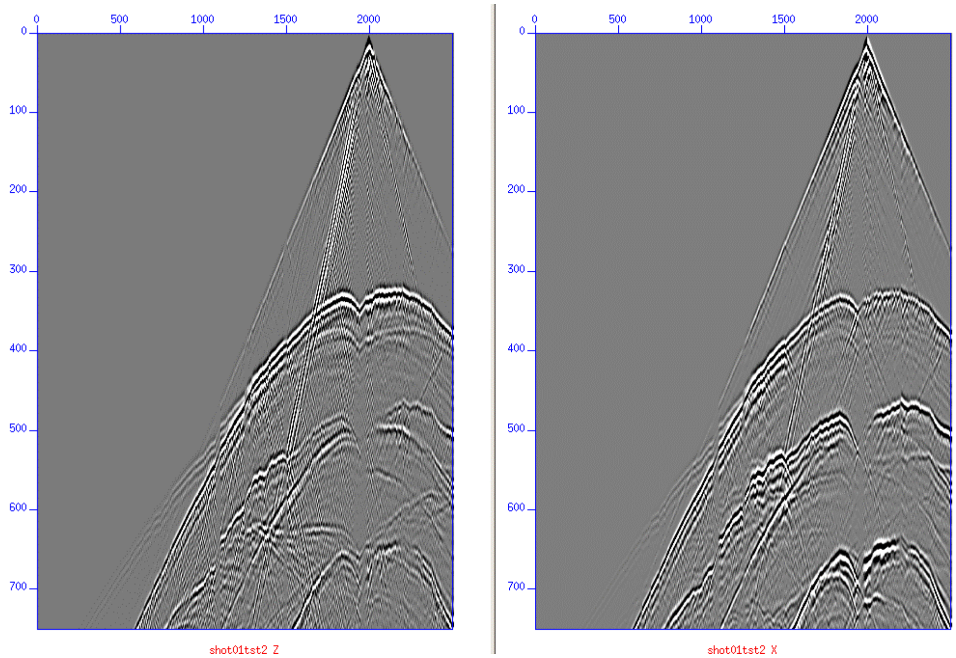

FIG. 13. Model without a low velocity layer. The vertical component is on the left and the horizontal component on the right.

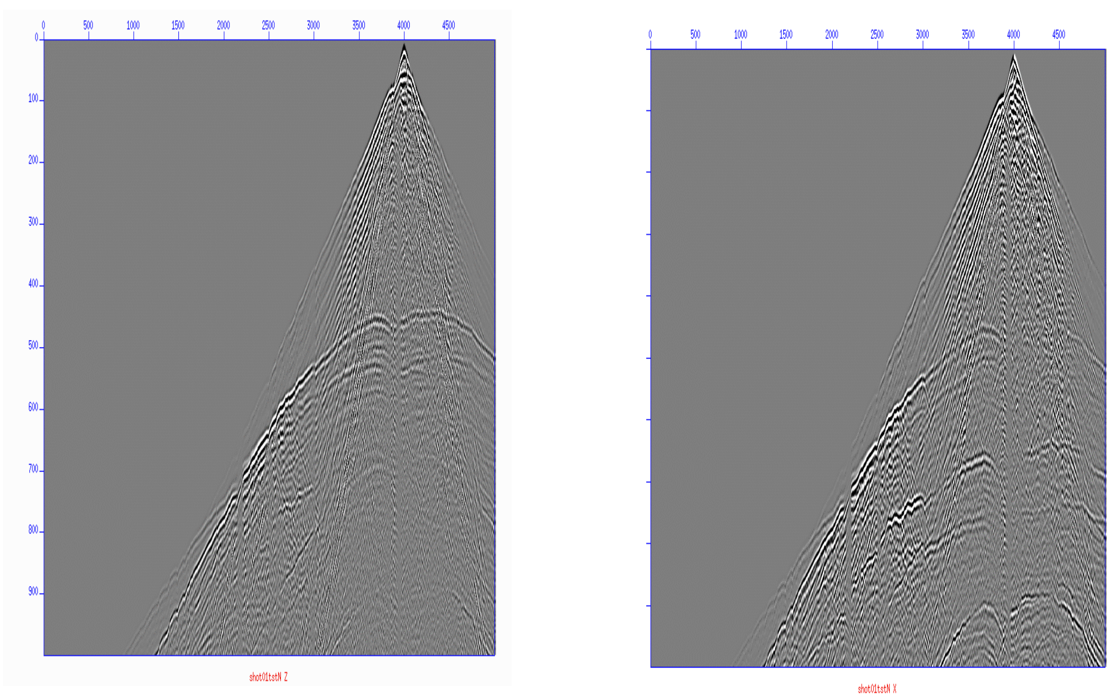

FIG. 14. Real topography with low velocity NSL. The vertical component is on the left and the horizontal on the right.

DISCUSSION

As shown by the models presented, the near surface low velocity layer can severely the information coming from the deeper reflectors, and creates strong, usually coherent noises that further obscure The character and amplitude of these events and distortions depend on the velocity properties of the near surface layer and its thickness. These events appear quite strong compared with many real data, which suggests a model of lesser velocity and thickness variation than the one usually assumed.

Finite difference is perhaps the modeling method most valued for its accurate representation of wave propagation. As such, all the wave modes are generated in agreement with the mathematical wave model assumed. However there are some limitations in the modeling program used here. It is based on a mathematical model which is elastic, 2D and isotropic; so amplitude inaccuracy can be expected compared with real data. Real data shows attenuation of high frequencies with time (anelasticity) and 3D geometrical spreading which are not present in our simulations.

In addition, its free surface solution is an approximation, taking into account that this method creates a staircase whose discrete steps actually represent a smooth real surface. Sometimes is difficult to distinguish the events generated by the wave propagation from the numerical artifacts created the computational model. As an example, the asymmetry observed in Figures 6 and 7 could be related to the relation between the directions of the seismic events and the finite difference grid. A finer grid can be a solution to some of these shortcomings; however the computational cost can become excessive. Some authors (e. g. Fuyuki and Matsumoto, 1980, and Robertsson, 1996) have proposed different approaches to the finite difference free surface calculation, which can be target of future research.

The free surface effect (Kähler and Meissner, 1985; Guevara, 2000) is another topic which requires additional considerations, since can create meaningful variation in seismic events and FD modelling appear as a quite appropriate tool to that purpose.

CONCLUSIONS

- The data sets show that the near surface layer generates many events that can obscure seismic events of interest.

- Compared with real data, some noticeable features can be observed in the modeling results: the noise generated at the surface appears quite strong, and first arrivals appear weaker.

- Some events usually not observed in real data can be attributed to the discretization process used in this algorithm.

- Because of the near surface properties it is difficult to observe shear or converted waves in many cases, which frequently happens in real data.

- High density spatial sampling is required for the low velocity events generated at the NSL.

- Subsurface reflections, for both P and S waves are strongly distorted by the near surface layer. This suggests that analysis of polarization and AVO will be very difficult in this context.

ACKNOWLEDGEMENTS

Thanks to Ecopetrol who allowed using the elastic modeling program, and to Felix Corboda, from Numerica Ltda (Colombia), who contributed to the development and adequacy of the modeling code to our requirements. Also thanks to the CREWES sponsors who supported this research.

REFERENCES

Anno, P. D., 1987, Two critical aspects of shear-wave analysis: statics solutions and reflection correlations, *in* Danbom, S. H. and Domenico, S. N., Editors, Shear wave exploration. SEG Geophysical development series, vol. **1**.

Cox, M. , 1999. Static corrections for seismic reflection surveys. SEG.

Flinn, E. A., 1965, Signal analysis using rectilinearity and direction of particle motion. Proceed. IEEE, **53**, pp. 1874-1876

Fuyuki M., and Matsumoto, Y. 1980 Finite Difference analysis of Rayleigh wave scattering at a Trench. Bulletin of the Seismological Society of America, Vol. **70**, No. 6, pp. 2051-2069, December 1980

Garotta, R., 2000. Shear-waves from acquisition to interpretation. SEG

Guevara, Saul E..,Margrave G. F. and Stewart, R. R. 2007. P-wave enhancement in rough terrain using multicomponent seismic data:Catatumbo, Colombia CSEG Annual Convention.

Guevara, Saul. 2000. Analysis and filtering of near-surface effects in land multicomponent seismic data. M Sc Thesis, University of Calgary.

Hayashi, K., Burns D. R., and M Nafi Toksôz M. N. 2001. Discontinuous-Grid Finite-Difference Seismic Modeling Including Surface Topography Bulletin of the Seismological Society of America, **91**, 6, pp. 1750–1764, December 2001z

Kähler, S. and Meissner, R. 1983. Radiation and receiver pattern of shear and compressional waves as a function of Poisson’s Ratio. Geophysical Prospecting **29**, p. 533-540.

Levander, A. R. 1988. Fourth-order finite-difference P-W seismograms. Geophysics, Vol. **53**. No. 11 (November 1988); P. 1425.-1436.

Molotova, L. V. and Vassil’ev, Y. I., 1960, Velocity ratio of longitudinal and transverse waves in rocks, II. Bulletin of the Academy of Sciences USSR - Geophysics Series, 731-743. (Translated by AGU)

Robertsson, J. O. A.. 1996. A numerical free-surface condition for elastic/viscoelastic finite-difference modeling in the presence of topography. Geophysics **61**, 1921-1934.